17th Mediterranean Conference on Control & Automation
Makedonia Palace, Thessaloniki, Greece
June 24 - 26, 2009

A Parametric Study on the Rolling Motion of Dynamically Running Quadrupeds During Pronking

Panagiotis Chatzakos and Evangelos Papadopoulos, *Senior Member, IEEE*

Abstract— **This paper examines the passive dynamics of straight-ahead level ground quadrupedal running and explores its use in formulating design guidelines that would: a) reduce steady-state roll and b) self-stabilize the rolling motion, thus making the control of the robot more straightforward. To study the effect of mechanical design in the rolling motion, a simple bounding-in-place (BIP) template is introduced as a candidate frontal plane model that captures the targeted steady-state behavior of a straight-ahead level ground running quadruped robot. This model is parametrically analyzed and local stability analysis shows that the dynamics of the open loop passive system alone can confer stability of the motion! These results might explain the success of simple, open loop running controllers on existing experimental robots and can be further used in developing control methodologies for legged robots that take advantage of the mechanical system.**

I. Introduction

LEGGED robots appear to be the best candidates for negotiating rough terrain. Animals exhibit impressive performance in handling rough terrain and hence they can reach a much larger fraction of the earth landmass on foot. However, their robotic counterparts have not yet benefited from the improved mobility and versatility that legs offer. Early attempts to design legged platforms resulted in slow, statically stable robots; see [1] for a survey. In this paper, however, we focus on dynamically stable legged robots. We seek to increase our understanding of the dynamics of straight-ahead level ground running, and hence increase our ability to develop fast and stable legged robots.

In an attempt to study the basic properties of sagittal plane running, Schwind proposed the Spring Loaded Inverted Pendulum (SLIP) template, which, despite its structural simplicity, was found to sufficiently encode the task-level behavior of animals and robots, [2]. Likewise, Schmitt and Holmes proposed the Lateral Leg Spring (LLS) template to analyze the horizontal dynamics of sprawled postured animals, [3]. Surprisingly they found that, despite its conservative nature, the LLS template exhibits some degree of asymptotic stability without the need of feedback control laws. In addition, recent research conducted independently by Seyfarth et al. ([4]) and Ghigliazza et al. ([5]) showed that when the SLIP is supplied with the appropriate initial conditions and for certain touchdown angles, not only does it follow a cyclic motion, but it also tolerates small perturbations without the need of a feedback control law.

This inherent stability of SLIP and LLS models is a very interesting property. Using such simple models and understanding how animal legs act like springs ([6]), i.e. absorbing part of the kinetic energy during touchdown and partially restoring it at liftoff ([7]), has encouraged or led directly to the design of many dynamic runners. Raibert set the stage with his groundbreaking work on dynamic legged locomotion by introducing one-, two- and four-legged robots, [8]. Later on, Buehler designed and built power autonomous legged robots with one, four and six legs, which demonstrate running in a dynamic fashion, [9]. Patrush and Tekken robotic quadrupeds by Kimura and co-workers are another successful example of dynamic locomotion, [10].

Besides the oscillations in the sagittal and horizontal planes, animals and dynamic robots of various morphologies typically exhibit rolling motions not captured in either the SLIP or LLS model. The observation of a roll component in legged locomotion has a long history in robotics, stretching back at least two decades, [11]. Various techniques, such as simple pelvic ([12]) or step-placement ([13]) feedback, can be shown to stabilize roll. Still, it appears that these controllers do not diminish its magnitude. Furthermore, it is generally accepted that roll in steady state legged gaits is not desired. As Koditschek and co-workers aptly suggest, such motion makes exteroceptive and even proprioceptive sensing more difficult, [14]. Visual data incurs a significant rotational overlay that necessitates extra processing; gyroscopic effects are harder to measure; and even tactile sensing by legs is complicated by alterations in touch-down timing arising from roll. From these perspectives, any design change that would reduce steady-state roll might seem to make the control of the robot more straightforward.

This work is co-funded by public (European Social Fund 80% and General Secretariat for Research and Technology 20%) and private funds (Zenon SA), within measure 8.3 of Op. Pr. Comp., 3rd CSP-PENED'03

In this paper, the passive dynamics of straight-ahead level ground quadrupedal running are examined and its use in

Panagiotis Chatzakos is with the Department of Mechanical Engineering, National Technical University of Athens, Greece (phone: +30-697-746-7158; e-mail: pchatzak@mail.ntua.gr).

Evangelos Papadopoulos is with the Department of Mechanical Engineering, National Technical University of Athens, Greece (phone: +30-210-772-1440; fax: +30-210-772-1450; e-mail: egpapado@central.ntua.gr).

formulating design guidelines that would reduce steady-state roll and self-stabilize the rolling motion are explored. To realize these goals, a simple bounding-in-place (BIP) template as a candidate frontal plane model is introduced in Section II. This model, which captures the targeted steady-state behavior of a straight-ahead running quadruped robot, is parametrically analyzed next. Numerical return map studies presented in Section IV reveal that passive generation of a large variety of cyclic motion is possible. Surprisingly, the local stability analysis in Section V shows that the dynamics of the open loop passive system alone can confer stability of the rolling motion. Findings and design guidelines that could assist in the design of new, and modifications of existing quadruped robots are drawn.

II. MODELING OF ROLLING

In this section, we propose a template for studying and analyzing rolling motion. This is inspired by SLIP, LLS and bounding model proposed by Buhler and coworkers, which exhibit natural stability. As in these simplified models, we assume rolling motion to be decoupled of pitching and yawing motions. In addition to the BIP model recently proposed in [14], which captures the salient aspects of a RHex-like robot frontal-plane roll, toe translation along horizontal plane is considered. We believe that this component is of significant importance to straight-ahead stable running. This model is shown in Fig. 1, while its parameters are given in Table 1.

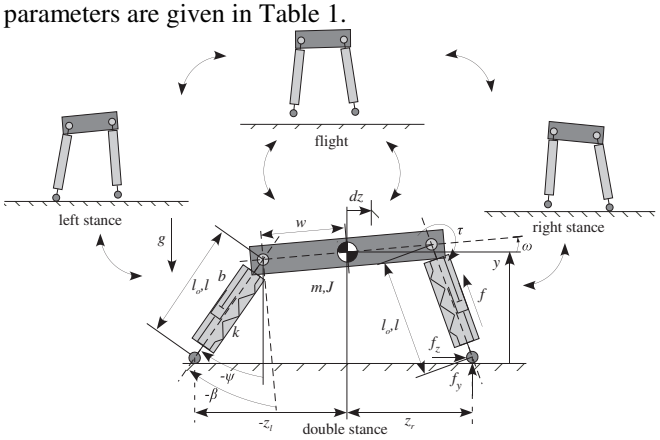

Fig. 1. Parameters of the template for straight-ahead level ground quadrupedal running and gait phases.

As shown in Fig. 1, the planar model represents the anterior of a quadruped, and consists of a rigid body and two springy massless legs, attached to either side of the body. Actuators control the angle of each leg with respect to the body and the torque delivered to each leg. Each leg represents either the front or the back leg that supports the body during the stance phase and includes friction modeling. Consequently, the gaits that can be studied employing this template are the two-beat ones, such as the curvet (front and rear legs move together), the amble (legs on the same side move together), the trot (diagonal legs move together) and the pronk (all legs move together). Particularly for the amble and pronk gaits, in which the two left or right legs are moving simultaneously, each modeled leg represents the left or the right leg pair and is called a virtual leg, [8]. Each virtual leg has twice the stiffness of the robot leg. The sum of forces applied on a virtual leg is double the ones on the real leg. The same rule holds for the joint torques.

TABLE I.
VARIABLES AND INDICES USED

Symbol	Variable	Symbol	Variable
z	COM horizontal pos.	h_{apex}	flight apex position
y	COM vertical pos.	g	gravity acceleration
ω	body pitch angle	m	body mass
β	leg absolute angle	J	body inertia
ψ	leg relative angle	w	hip to COM distance
z_l	left toe horizontal pos.	r	as an index: right leg
x_r	right toe horiz. pos.	l	as an index: left leg
l	leg length	j	dimensionless inertia
l_o	leg rest length	r	relative leg stiffness
k	leg spring stiffness	q	half hip separation
τ	torque delivered at hip	Fr	Froude number
f	axial force at leg	s	time scale
b	damping coefficient	*	dimensionless

In this work, we are primarily interested in providing design guidelines that would reduce steady-state roll during pronk. Since this is the gait with the least (practically) oscillation in the sagittal plane, we believe that pronk is a candidate well suited for robotic locomotion as it would make exteroceptive and even proprioceptive sensing less difficult and the control of the robot more straightforward. Visual data would incur a minimal rolling and pitching overlay, gyroscopic effects would be easier to measure and even tactile sensing by legs would be less complicated as there would be only few alterations in touch-down timing.

System dynamics are derived using a Lagrangian formulation, with generalized coordinates to be the Cartesian variables describing the center of mass (COM) position and the main body's attitude. During flight, the robot is under the influence of gravity only. Throughout the stance phase, the robot's toes are fixed on the ground, and act as lossless pivot joints. The dynamics for any phase may be derived from that of the double stance, by removing appropriate terms. Hence, only the double stance dynamics is given here, in the form of a set of differential and algebraic equations,

$$m\ddot{z} = -\left(k\left(l_o - l_l\right) - b\dot{l}_l\right)\sin\beta_l - \tau_l\cos\beta_l/l_l - \\ -\left(k\left(l_o - l_r\right) - b\dot{l}_r\right)\sin\beta_r - \tau_r\cos\beta_r/l_r \quad (1)$$

$$m\ddot{y} = \left(k\left(l_o - l_l\right) - b\dot{l}_l\right)\cos\beta_l - \tau_l\sin\beta_l/l_l + \\ +\left(k\left(l_o - l_r\right) - b\dot{l}_r\right)\cos\beta_r - \tau_r\sin\beta_r/l_r - mg \quad (2)$$

$$J\ddot{\omega} = \tau_l - w\left(k\left(l_o - l_l\right) - b\dot{l}_l\right)\cos\left(\beta_l - \omega\right) + \\ +\tau_r + w\left(k\left(l_o - l_r\right) - b\dot{l}_r\right)\cos\left(\beta_r - \omega\right) + \\ +w\tau_l\sin\left(\beta_l - \omega\right)/l_l - w\tau_r\sin\left(\beta_r - \omega\right)/l_r \quad (3)$$

where

$$\beta_l = \text{atan2}\left(y - w\sin\omega, z_l + w\cos\omega\right)$$
$$\beta_r = \text{atan2}\left(y + w\sin\omega, z_r - w\cos\omega\right) \quad (4)$$

$$l_l = \sqrt{\left(z_l + w\cos\omega\right)^2 + \left(w\sin\omega - y\right)^2}$$
$$l_r = \sqrt{\left(z_r - w\cos\omega\right)^2 + \left(w\sin\omega + y\right)^2} \quad (5)$$

III. NON-DIMENSIONAL DYNAMICS

The set of Eqs (1)-(5) is manipulated next to become independent of the choice of units, i.e. dimensionless. The non-dimensional variables are formed in ways that define the morphology of the quadruped robot or that correspond to ratios of robot physical parameters in the model equations. To achieve that, the following dimensionless variables are introduced,

$$t^* = t/s \quad (6)$$

$$z^* = z/l_o\,,\ \dot{z}^* = s\,\dot{z}/l_o\,,\ \ddot{z}^* = s^2\,\ddot{z}/l_o \quad (7)$$

$$y^* = y/l_o\,,\ \dot{y}^* = s\,\dot{y}/l_o\,,\ \ddot{y}^* = s^2\,\ddot{y}/l_o \quad (8)$$

$$\omega^* = \omega,\ \dot{\omega}^* = s\,\dot{\omega},\ \ddot{\omega}^* = s^2\,\ddot{\omega} \quad (9)$$

where s is the time scale of the system, and the rest of the variables are defined in Table 1.

By substituting (6)-(9) into the equations of motion, one gets a dimensionless description of the system. The resulting motion of the COM is then characterized by a time scale, which is associated to the inverse of the natural frequency of the horizontal motion,

$$s^2 g/l_o = 1 \Rightarrow s = \sqrt{l_o/g} \quad (10)$$

While the individual dimensionless equations would be different if one uses a different time scale, the relationships between them would be invariant.

Selection of the time scale as in (10), results to a number of dimensionless parameter groups, which are widely used by experimental biologists and roboticists. These include: (a) the Froude number Fr ([15]), defined as

$$Fr = v/\sqrt{g\,l_o} \quad (11)$$

where v is the robot horizontal speed, (b) the dimensionless inertia j ([8]), i.e. the robot's body inertia normalized to mw^2,

$$j = J/m\,w^2 \quad (12)$$

and (c) the leg relative stiffness r ([6]), which is given as

$$r = k\,l_o/m\,g\,. \quad (13)$$

Also, the following dimensionless parameters are introduced: (a) the normalized half hip separation q

$$q = w/l_o \quad (14)$$

and (b) the dimensionless viscous friction coefficient b^*

$$b^* = b/m\sqrt{l_o/g} \text{ or } b^* = 2\zeta\sqrt{r} \quad (15)$$

where ζ is the damping ratio.

Force and torque variables are finally normalized as

$$f_i^* = f_i/mg\,, i = l, r \text{ and } \tau_i^* = \tau_i/mg\,l_o\,, i = l, r. \quad (16)$$

IV. PASSIVE ROLLING CYCLES

The goals of the analysis are to determine the conditions required to permit steady state cyclic motion and to find ways to apply these results to facilitate improved quadruped robots design. The fact that there exist examples of dynamic systems that encode the target behavior of running animals and robots with inherent stability, which not only do they follow a cyclic motion when supplied with the appropriate initial conditions and for certain touchdown angles, but they also tolerate small perturbations without the need of a feedback control law, motivated us to study the passive dynamics (the unforced response of the system under a set of initial conditions); see a recent example in [16]. Practically, if the system remains close to its passive behavior, then active stabilization may not be required or may require less control effort and sensing. Furthermore, the actuators have less work to do to maintain the motion and energy efficiency is improved, an important issue in mobile robots.

The unactuated and conservative model that is used in our analysis is derived from the dimensionless description of the system by eliminating actuation and energy dissipation terms. An analytical account of this hybrid, tightly coupled, nonlinear dynamical model promises to be very complicated and lies well beyond the scope of the present paper. Instead, we turn to numerical simulations to study the system's behavior. We used numerical simulations to generate system trajectories from a variety of initial conditions. In particular, we searched for equilibrium gaits (defined as periodic orbits of the hybrid dynamical system). To formulate these gaits, we employ a Poincaré Map technique, [16]. The return map connects the system state at a well-defined locomotion event to the state of the same event at the next cycle. Here, this event is chosen to be the apex height. We could select any other point in the cycle. However, the vertical velocity at apex height is always zero, which reduces the dimensions of the state vector. A second dimensional reduction to the state vector can be obtained by projecting out the horizontal component z of the state vector, since it is not relevant to describing the running gait. Thus, the state vector x* at apex height is given as,

$$\mathbf{x}^* = \begin{bmatrix} y^* & \omega^* & \dot{z}^* & \dot{\omega}^* \end{bmatrix}. \quad (17)$$

The state vector at apex height for some cycle n, $\mathbf{x}_n^*$, constitutes the initial conditions. Based on these, the flight equations are integrated until one of the touchdown events occurs, e.g., left or right leg stance. The touchdown event triggers the next phase, whose dynamics are integrated using as initial conditions the final conditions of the previous state. Successive forward integration of the dynamic equations of all the phases yields the state vector at apex height of the next stride, which is the value of the Poincaré return map F. If the state vector at the new apex height is identical to the initial one, the cycle is repetitive and yields a fixed point. Mathematically, this is given as

$$\mathbf{x}^*_{n+1} = \mathbf{F}\left(\mathbf{x}^*_n, u^*_n\right) \quad (18)$$

where $\mathbf{u}^*=[\beta^*_{l,td}\ \beta^*_{r,td}]$ includes the inputs, which are the touchdown angles, left and right leg.

Although touchdown angles are not part of state vector and they do not participate in the dynamics, they directly affect the value of the return map as they determine touchdown and liftoff events and impose constraints on the motion of robot during left leg, right leg and double stance phases.

In order to determine the conditions required to result in steady state cyclic motions, we resort to a numerical evaluation of the return map using a Newton-Raphson method. By employing this method, a large number of fixed points can be found for different initial conditions and different touchdown angles. Variant dimensionless combinations of robot's physical parameters, as defined in (12)-(14), also result to different fixed points. These design parameters vary between their extreme values found in experimental biology references, [17] and [18], as follows,

$$j = 0.80 - 1.25,\ r = 10 - 30,\ q = 0.2 - 1.2 \quad (19)$$

In Fig. 2 plots showing the evolution of the states during one cycle of the rolling motion corresponding to a fixed point are presented.

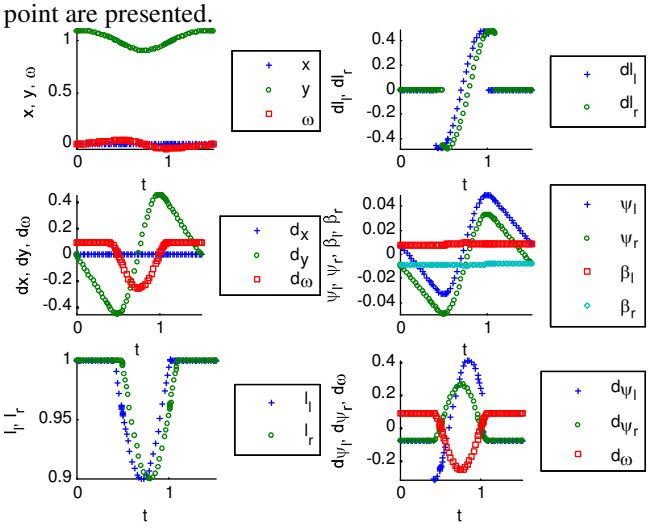

Fig. 2. Evolution of the state variables during one passive rolling cycle, corresponding to a fixed point.

Fig. 3 displays the sum of the leg touchdown angles, defined as (β_l+β_r), at fixed points for varying relative stiffness r (x axis) and normalized body width q (y axis) and for a range of dimensionless body inertia j (upper row) and roll rate (lower row). It can be seen that there is a continuum of fixed points, which follows different patterns for high and low roll rate. As it can be seen from Fig. 3, the sum of touchdown angles that corresponds to high roll rate is large. This means that the robot must extend its right and left legs to a great degree outwards in order to maintain the rolling motion and keep running, which is practically difficult to achieve as slipping might occur. As expected, low roll rate requires only a small sum of touchdown angles.

Finding 1. High roll rate generally necessitates large touchdown angles to stabilize the rolling motion. Contrarily, touchdown angles at low roll rate remains relatively small.

Furthermore, it appears that the effect of dimensionless body inertia j is significant to the sum of the touchdown angles. Unit dimensionless body inertia (j=1) requires the least extension of the right and left legs to the side in order to maintain the rolling motion compared to larger values of j. We must note here that it was not possible to find fixed points for dimensionless body inertia of less than one (j<1). This finding is in accordance with the findings in [14], where Koditschek and co-workers studied the frontal plane disturbance recovery patterns of the conservative version of EduBot, a hexapedal RHex-like robot. No matter how stringent their error tolerances were, they always found the equilibrium gaits to be unstable. The instability observed is unmistakably due to the magnitude of the dimensionless body inertia, which is less than one.

Finding 2. Dimensionless inertia more than one mostly results to large touchdown angles over the whole range of roll rate. For a specific roll rate, touchdown angles become least when the dimensionless body inertia is equal to one. When the dimensionless body inertia is less than one, it is unlikely rolling motion to be passively stable.

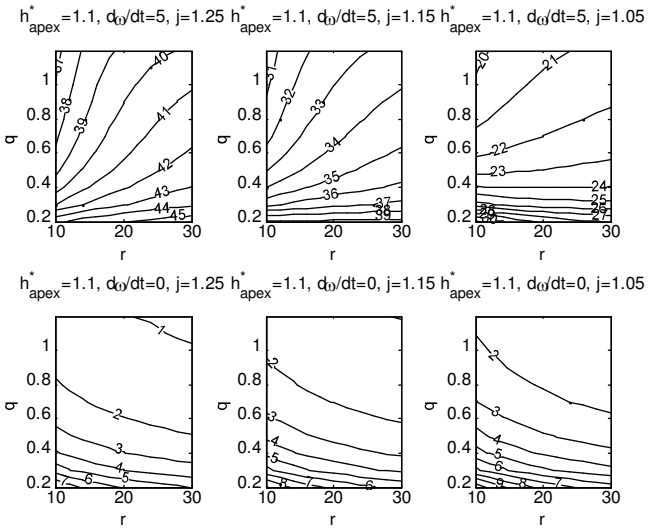

Fig. 3. Sum of the leg touchdown angles (deg), for varying dimensionless robot parameters and roll rate.

From Fig. 3 it is also evident that the effect of normalized body width q is significant to the sum of the touchdown angles in any case, at high or low roll rate and various dimensionless inertias. As reasonably expected, for wider (compared to hip height) body configurations (q→1), it is easier to maintain straight ahead running, i.e. the robot must extend its right and left legs to a less degree outwards in order to maintain the rolling motion. As it can be seen from Fig. 3 for low normalized width values (q→0.2), the sum of touchdown angles is relatively large, especially at its extreme value (q=0.2).

Finding 3. Wide, compared to hip height, body configuration is generally preferred when it comes to how

much effort is required to stabilize rolling motion and to keep straight ahead running, given that dimensionless inertia remains more than or equal to one.

Finally, equally significant is the effect of relative leg stiffness *r*, as Fig. 3 depicts. It is interesting that the effect of *r* is contradictory for high and low roll rate. For high roll rate, the sum of touchdown angles is increasing function of relative leg stiffness, while for low roll rate is decreasing. It also appears that the effect of relative leg stiffness is independent of the magnitude of dimensionless body inertia. Therefore, relative leg stiffness should be large since most of the times low roll rate are desired.

Finding 4. The effect of leg relative stiffness is independent of dimensionless body inertia and contradicting at high and low roll rate. To keep the effort of maintaining rolling motion the least possible, leg relative stiffness should be low for high roll rate and large for low roll rate.

V. STABILITY OF PASSIVE ROLLING

The existence of passively generated running cycles is by itself a very important result since it shows that such a complex activity can be simply a natural motion of the system. However, in real situations the robot is continuously perturbed, therefore, if the fixed point were unstable, then the periodic motion would not be sustainable. Hence, it is therefore important to study the stability properties of the fixed points found above and to identify robot physical parameters that improve the robustness of the system against perturbations. We characterize the stability of the fixed points using the eigenvalues of the linearized return map. For that, we assume that the apex height states are perturbed from their steady-cycle values, by some small amount $\Delta\mathbf{x}$. The model that relates the deviations from steady state, i.e. the incremental or small-signal model, is

$$\Delta\mathbf{x}^*_{n+1} = \left.\frac{\partial\mathbf{F}(\mathbf{x}^*,\mathbf{u}^*)}{\partial\mathbf{x}}\right|_{\mathbf{x}=\bar{\mathbf{x}}} \Delta\mathbf{x}^*_n + \left.\frac{\partial\mathbf{F}(\mathbf{x}^*,\mathbf{u}^*)}{\partial\mathbf{x}}\right|_{\mathbf{u}=\bar{\mathbf{u}}} \Delta\mathbf{u}^*_n \quad (20)$$

with $\Delta\mathbf{x}^* = \mathbf{x}^* - \bar{\mathbf{x}}^*$ and $\Delta\mathbf{u}^* = \mathbf{u}^* - \bar{\mathbf{u}}^*$.

For small perturbations, the apex height states at the next stride can be calculated by (20), which is a linear difference equation. If all the eigenvalues of the system matrix $\mathbf{A}$,

$$\mathbf{A} = \partial\mathbf{F}(\mathbf{x}^*,\mathbf{u}^*)/\partial\mathbf{x}\Big|_{\mathbf{x}=\bar{\mathbf{x}}} \quad (21)$$

have magnitude less than one, then the periodic solution is stable and disturbances decay in subsequent steps. If not, disturbances grow and eventually repetitive motion is lost.

Fig. 4 shows the eigenvalues of matrix $\mathbf{A}$ for varying leg relative stiffness. Note that the same pattern is observed for different roll rates and apex heights. As it was expected, one of the eigenvalues is always located at zero, representing the fact that the system is conservative. Two of the eigenvalues start on the rim of the unit circle, and as relative leg stiffness increases they move towards each other, they meet on the real axis and finally they move again towards the rim of the unit circle. The third eigenvalue starts at a high value and moves towards the unit circle and finally it gets into it, for specific values of relative leg stiffness, while the other two eigenvalues remain well behaved. Therefore, there is region of parameters where the system is passively stable. This is a very important result since it shows that the system can tolerate small perturbations of the nominal conditions without any control action taken! This fact could provide a possible explanation to why existing experimental robots can run, without the need of complex state feedback. It is important to mention that this result is in agreement with recent research from biomechanics, which shows that when animals run at high speed, passive dynamic self-stabilization from a feed-forward, tuned mechanical system can reject rapid perturbations and simplify control, [19].

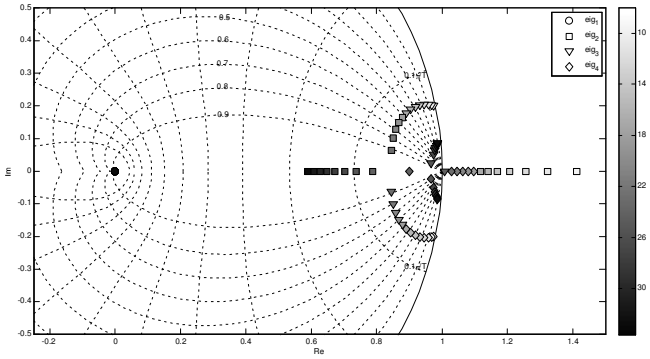

Fig. 4. Root locus showing the paths of the four eigenvalues as leg relative stiffness *r* increases.

VI. STABILITY AND DESIGN GUIDELINES

Using this systematic procedure for finding stable fixed points described previously, conclusions on how the system responds under a set of initial conditions and design parameters can be drawn. The purpose of the analysis in this section is to quantify the properties of passively generated periodic rolling motion for quadruped robots and to search for regions where the system can passively tolerate departures from the fixed points.

To show how motion characteristics and design parameters affect the stability of the motion, we present figures that display isolines of the magnitude of the larger eigenvalue of system matrix $\mathbf{A}$. The largest eigenvalue norm is interpreted as heights with respect to the x-y plane, where x-y variables are either motion characteristics, i.e. the roll rate, or the dimensionless combinations of robot physical parameters defined in (13) and (14), e.g. leg relative stiffness *r* and normalized half hip separation *q*. For certain values of these variables the larger eigenvalue enters the unit circle, while the other eigenvalues remain well behaved. This fact shows that, for these parameter values, the system is self-stabilized. In all figures, the grey hatched area corresponds to unstable regions, i.e., regions where at least one eigenvalue is located outside of the unit circle and the system is not passively stable. The magnitude of the "non-

participating" variables is shown in the title of each subplot.

To this end, isolines of the largest eigenvalue norm at various pitch rates and values of dimensionless inertia are displayed in Fig. 5. The contour plots are drawn for dimensionless apex height h_{apex}=1.1, dimensionless body inertia j=1, and varying roll rate. It can be seen that the lower the relative leg stiffness is, the less unstable the system is, especially at high roll rate; for those specific values of our experiment the minimum relative leg stiffness is 14, i.e., r>14, for the system to be self-stable, that is stable without the need of a closed loop controller. Also, lowering the normalized body width q, mostly at high roll rate helps expanding the range of leg relative stiffness, for which the system is passively stable. Nonetheless, q has only minor effect to the stability of rolling motion.

Finding 5. Relative leg stiffness should be above a certain threshold to stabilize rolling motion. At high roll rate, low normalized body width prevents this threshold to increase.

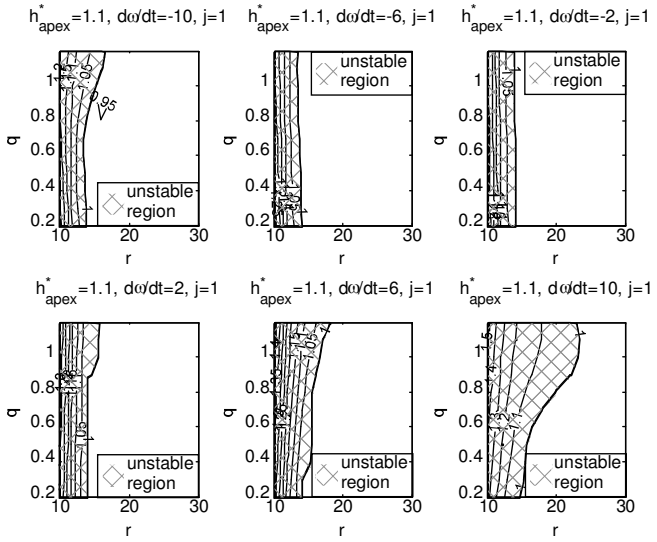

Fig. 5. Largest eigenvalue norm for varying roll rate, relative leg stiffness and normalized body width.

In conjunction to [20], where results about the stability of the passive dynamics of a quadruped robot running in the sagittal plane with a pronking gait are presented, we conclude that a quadruped robot with dimensional body inertia (both longitudinal and traversal) j equal to one (j=1), low length-to-hip height ratio p (0.3<p<0.5) and width-to-hip height ratio q (0.4<q<0.6) and moderate relative leg stiffness (14<r<18) could be able to perform self-stable straight-ahead level ground running behavior in significantly broader ranges of forward speed.

VII. Consclusion

he stability analysis of the passive dynamics of straight-ahead level ground quadrupedal running was studied in a dimensionless context. A simple bounding-in-place (BIP) template as a candidate frontal plane model was introduced and parametrically analyzed. It was shown that mechanical design can provide self-stabilizing characteristics to the quadruped robot against external perturbations and result to dynamically stable rolling motion, with physically realistic roll rate, for the two-beat gaits, such as the curvet, the amble, the trot and the pronk. We anticipate that the proposed guidelines will assist in the design of new, and modification of existing quadruped robots. These can be summarized as: (a) dimensionless body inertia should be larger than one to enable passive rolling motion, and ideally equal to one to confer passive stability of the rolling motion, (b) wide body configurations reduce the effort required to maintain rolling motion, and (c) relative leg stiffness contributes to the stability of the open loop system and should be above a certain threshold, which depends on specific parameters of the system and roll rate.

References

[1] Berns K., *Walking Machine Catalogue*, www.walking-machines.org/.

[2] Schwind W. "Spring Loaded Inverted Pendulum Running: A Plant Model", *PhD Thesis*. University of Michigan, MI, USA, 1998.

[3] Schmitt J. and Holmes P., "Mechanical models for insect locomotion: Dynamics and stability in the horizontal plane I. Theory". *Biological Cybernetics*, 83(6):501–515, 2000.

[4] Seyfarth A., Geyer H., Guenther M. and Blickhan R., "A Movement Criterion for Running", *J. of Biomechanics*, 35(5): 649-655, 2002.

[5] Ghigliazza R. M., Altendorfer R., Holmes P. and Koditschek D. E., "A Simply Stabilized Running Model", *SIAM J. of Applied Dynamical Systems*, 2(2): 187-218, 2003.

[6] Blickhan R., "The spring-mass model for running and hopping", *J. of Biomechanics*. 22(11-12), 1989, pp: 1217–1227.

[7] Cavagna G. A., Heglund N. C., and Taylor C. R., "Mechanical work in terrestrial locomotion: Two basic mechanisms for minimizing energy expenditure", *J. of Physiology*, 233(5):243-261, 1977.

[8] Raibert M. H., "Legged Robots that Balance", MIT Press, MA, 1986.

[9] Buehler M., "Dynamic Locomotion with One, Four and Six-Legged Robots", *J. of the Robotics Society of Japan*, 20(3):15-20, 2002.

[10] Kimura, H. Fukuoka Y. and Cohen A. H., "Adaptive Dynamic Walking of Quadruped Robot on Natural Ground Based on Biological Concepts", *Int. J. of Robotics Research*, 26(5): 475-490, 2007.

[11] Glower J. and Ozguner U., "Control of a quadruped trot", *IEEE Int. Conf. on Robotics and Automation*, 3:1496-1501, 1986.

[12] Wisse M., Schwab A. L. and Linde R. Q., "A 3d passive dynamic biped with yaw and roll compensation", *Robotica*, 19:275–284, 2001.

[13] Kuo A. D., "Stabilization of lateral motion in passive dynamic walking", *Int.J. of Robotics Research*, 18:917–930, 1999.

[14] Burden S., Clark J., Weingarten J., Komsuoglu H. and Koditschek D., "Heterogeneous Leg Stiffness and Roll in Dynamic Running", *IEEE Int. Conf. on Robotics and Automation*, 1:4645-4652, 2007.

[15] Alexander R. McN, "Terrestrial Locomotion", *Mechanics and Energetics of Animal 1ocomotion*, Chapman and Hall, London, 1977.

[16] Poulakakis, I. Papadopoulos E. G. and Buehler M., "On the Stability of the Passive Dynamics of Quadrupedal Running with a Bounding Gait", *Int. J. of Robotics Research*, 25(7): 669-687, 2006.

[17] Farley C.T., Glasheen J., and McMahon T.A., "Running Springs: Speed and Animal Size", *J. of Exp. Biology*, 185: 71-86, 1993.

[18] Herr H. M., Huang G.T. and McMahon T. A., "A model of scale effects in mammalian quadrupedal running", *J. of Exp. Biology*,205: 959-967, 2002

[19] Kubow T. and Full R., "The Role of the Mechanical System in Control: A Hypothesis of Self-stabilization in Hexapedal Runners" *Phil. Trans. of the Royal Society B*, 354(1385): 854-862, 1999.

[20] Chatzakos, P. and Papadopoulos, E., "Dynamically Running Quadrupeds Self-Stable Region Expansion by Mechanical Design," *IEEE Int. Conf. on Robotics and Automation*, May 2009, Japan.